

Adjustment and Application of the Band Gap of Nano Titanium Dioxide: Its Usefulness on Photo degradation of Wastewater (phenol)

Moatasem AlSalih^{1*}, Syakirah Samsudin², Seenaa Wdaah AlSalih³

Biology department, Faculty of Science and Mathematics, University Pendidikan Sultan Idris(UPSI), Tanjong Malim Perak, Malaysia.

*Corresponding Author: alsalihmoatasem@gmail.com

ARTICLE INFO

Article History:

Received: June 9, 2021

Accepted: June 19, 2021

Online: June 29, 2021

Keywords:

Pt-doped-TiO₂,
sol-gel method,
photodegradation,
photocatalysis,
AFM,
XRD

ABSTRACT

A high concentration of phenol and its derivatives were found in the surface water of the Euphrates River in south Iraq's Nasiriya city causing its pollution from the wastewater derived from different chemicals. This study includes modification of the TiO₂ (anatase) bandgap by doping with platinum atoms using the sol-gel method. The modification would reduce the gap separating energy levels between conduction band CB and valence band VB, which in turn, would facilitate the transfer of excited electrons from VB to CB. Absorption of the energy from incident photons having the same or larger energy than that of the bandgap would promote the formation of the couple (electron-hole). The resulting (e⁻/h⁺) couple would act to produce ([•]OH) radicals. [•]OH radicals have a power with full capacity to destroy organic pollutants in the water that are absorbed on the surface of the photocatalytic TiO₂. The structure of prepared TiO₂ powders was characterized using XRD, the particle size and their distribution were characterized using Atomic Force Microscopy (AFM). The photocatalytic reaction was followed out using ATR-FTIR, UV-Vis spectrophotometry. The effect of the weight of the photocatalytic catalyst (TiO₂) from (0.10 – 0.83 g. L⁻¹) was studied to monitor its effect on the rate of decomposition of phenol on the pre-determined aqueous solution of the compound. The most effective weight was found to equal (0.43 g. L⁻¹). The activities of TiO₂ (anatase) and doped TiO₂ with platinum were studied under the influence of a source of UV light and direct sunlight under the same conditions. The results revealed that the reaction obeys first-order kinetics having a rate constant of 4.69x10⁻⁶ min⁻¹ for TiO₂ and 9.44x10⁻⁶ min⁻¹ for doped TiO₂.

INTRODUCTION

The Euphrates River passes through Nasiriyah, the largest city in southern Iraq. River basin is a major source of water supply for many purposes and provides fertile lands, which supports the development of highly populated residential areas due to its favorable conditions (Black, 2016). Due to the primacy of water-borne trade, human settlements and industry have traditionally been stationed along rivers, estuaries, and coastal zones. The water quality of a river is a composite of various interconnected

compounds that are subject to local and temporal fluctuations and are also influenced by the amount of water flow (**Mandal et al., 2010**). Rivers are also the predominant inland water body for domestic, industrial, and agricultural operations, and they frequently transport considerable amounts of municipal sewage, industrial wastewater discharges, and seasonal runoff from agricultural fields (**Singh et al., 2004; Pradhan et al., 2009; Hu et al., 2011**). The surface waters have been sullied because of the releases of wastewater containing degradable organics, supplements and homegrown emanating. Notably, river water contamination can be connected to the kind of wastewater delivered by metropolitan, modern, and rural activities and released into surface and subsurface waters (**Vittori et al., 2010**). The increment in human populace and financial activities have filled in scale; the requests for huge scope providers of freshwater from different contending end clients have expanded colossally. The decrease in the quality and amount of surface water assets can be credited to water contamination and the ill-advised administration of the asset (**Mustapha and Nabegu 2011**). Numerous territories throughout the world are influenced at the same time by urbanization processes, industrial and agricultural operations, and many cities in emerging countries were built without enough or proper planning. This resulted in indiscriminate behavior, such as throwing rubbish into bodies of water and washing and bathing in open surface water bodies (**Cukrov et al., 2012**). The deterioration of water quality has far-reaching effects on human, animal, and plant life. It is critical to determine those sources and their contribution to an area's total pollution from an environmental, economic, and/or social standpoint (**Tobiszewski et al., 2010**). As of late, there has been an expanding attention to, and worry about, surface water contamination everywhere in the world, and new methodologies toward the wellsprings of toxins, and accomplishing practical abuse of water assets have been created. The joined utilization of natural devices, for example, multivariate measurable procedures empower the order of water tests into particular gatherings, source allocations, relationship, and contrast in the boundaries utilized dependent on hydrochemical attributes (**Shrestha et al., 2008**). They more properly reflect the multivariate nature of the natural environment, allowing for the handling of huge datasets with a large number of parameters by summarizing the redundancy and discovering and characterizing really multivariate patterns in the datasets (**McGarigal et al., 2000**). The use of conventional techniques of descriptive analysis to interpret surface water quality has several limitations of not detecting the long-term correlation between variables and poor delineation in the source apportionments of the surface water quality variability. Through using of environmetric technique, the results obtained for the removal of phenol from water by a new model nanoparticles generator are presented in this study. In all cases, the concentration of corresponding phenol was measured before and after nanoparticles irradiation treatment of water (**Darabdhara et al., 2016**), exposures, dissolved, sprays with nanoparticles (NP) to protect plants against Fusarium wilt (**Dimkpa et al., 2018**), standard methods were used to determine for the experiments

were carried out in a laboratory setting. Normally, the scale-up was anticipated with the ultimate goal of using this type of nanoparticles for phenol removal in waterworks. Such applications are required in Iraq and Egypt, as well as possibly other countries because river basins have extensive water sources (**Spath and Dayton, 2003; Chenier, 2012**).

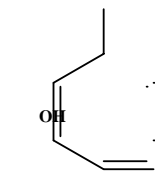
In various countries, high concentrations of phenols, for example, in the stream Euphrates, caused by random infrastructure planning (for the most part from coal thermal electrical energy stations and Industrial waste), as well as wastewater often hinder the creation of drinking water stations at a few towns in southern Iraq (**Abdullah, 2013; Ewaid, and Abed, 2017; Abbas, and Hassan, 2018; Das *et al.*, 2020**). Representations of the death phenomena of fish, phytoplankton and plants in rivers were abundant. Water scarcity could last for several weeks in some cases (**Vione *et al.*, 2018**). The greatest permitted centralization of phenols in stream water in Iraq and Syria is 0.01 mg/L, however determine phenols levels, it was represent a higher significantly. Packaged drinking water ought not contain phenols while other drinking water could contain up to 0.001 mg/L (like in certain nations). Remarkably, phenol evacuation has likewise been examined as pesticide disintegration item in stream water (**Dimkpa *et al.*, 2018; Levchuk *et al.*, 2018; Yoon *et al.*, 2020**).

Phenol

Phenol is classified as an aromatic compound, and a OH bunch is straightforwardly connected to a benzene ring as demonstrated in Table (1). Unadulterated phenol is a white strong glasslike, sanitizer smelling. Often the crystals are rather humid and colorless. The solubility of phenol in water is limited. It has a slight acidic flavor. Its molecule has a low tendency, the H^+ ion is removed from the hydroxyl group, resulting in the extremely water-soluble phenoxide anion $\text{C}_6\text{H}_5\text{O}$. Furthermore, substantial amounts of phenol and its derivatives have been discovered in nature, indicating natural contamination (**Rappoport, 2004; Karim and Fakhruddin, 2012**).

Waste water originated from various chemical industries such as resin production, petrochemical industry, oil refinery and the production of paper as well as iron smelting contaminate water sources. Phenol, on the other hand, is highly corrosive and moderately toxic. It has a variety of harmful effects on human beings with respect to burning the skin and other tissues with which it comes into contact. If the human body got inhaled, severe skin burns and interior corrosion would come to surface (**Hashimoto *et al.*, 2005; Paramasivam *et al.*, 2012**). In this context, the current study was conducted to provide a comprehensive data on the dangerous extensive distribution of the phenols compounds .

Table 1: The structure and general properties of phenol.

Structure	Molecular formula	Molecular weight (g/mol)	Properties	
			Melting point (K)	Boiling point (K)
	C ₆ H ₅ OH	94.11	313.5	454.7

Source: (Rappoport, 2004)

Titanium dioxide (TiO₂) photocatalytic semiconductor is the most attractive environmental purification tool due to its outstanding desirable characteristics. In this essence, the TiO₂ semiconductor absorbs a little fraction of the solar spectrum in the UV region. Nowadays, titanium dioxide (TiO₂) has widely gained a great deal of attention because of its chemical stability, non-toxicity, low cost, and other advantageous properties. Therefore, it has been worldly used in applications such as photovoltaic cells, photocatalysis, environmental purification, photoinduced super hydrophilicity as well as an ingredient in a pigment. With respect to photocatalysis, TiO₂ is close to being an ideal photocatalyst due to its aforementioned properties. Generally, both anatase and rutile are used as photocatalysts and some research stated that anatase had higher photoactivity than rutile (bandgap energy of anatase TiO₂ is 3.2eV, 384nm, and 3.02 ev, 411nm, for rutile TiO₂)(**Kim et al., 2005; Rashed and El-Amin, 2007; Schulze and Schmidt, 2015**). As a result, changing the absorption threshold to the visible zone is critical for obtaining energy from the sun. Thus, the change in TiO₂ to make it a visible light and sensitive was one of the most important aims to enhance TiO₂'s utility. In order to achieve this, many techniques have been proposed. Previous studies examined transition metal doping Fe, Ni,(**Pan et al 2016; Wu et al ., 2019; Zhu et al.,2020**)and Cr into TiO₂, (**Pan, and Wu, 2006; Gönüllü, et al., 2015**). This can increase visible light absorption but those materials are thermally unstable and have increased carrier recombination, Pt centers (**Kim et al., 2005**). Non-metal atoms have recently been doped N, S, and C into the TiO₂. There are five major points of view on the modification mechanism of TiO₂ doped with Pt. The majority of the Pt ions substituted in the TiO₂ lattice were in the Pt(IV) form, with some Pt(II) on the sample surface. PtionTiO₂ demonstrated stronger photocatalytic activity than undoped TiO₂ when exposed to UV light (**Kim et al., 2005; Rashed and El-Amin, 2007; Zhang et al., 2015**). Additionally, The visible light behavior of Ption-TiO₂ was significantly influenced by the calcination temperature and concentration of Pt ion dopant, which were optimum at 673 K and 0.5 atom percent, respectively. Since their energies are so similar, Pt ²p state hybrids with O ²p states in anatase TiO₂ doped with platinum degraded Bandgap narrowing found Pt 2p state hybrids with O ²p states in anatase TiO₂ doped with platinum, and thus the band gap of Pt-TiO₂ is narrowed and becomes able to absorb visible light. TiO₂ oxygen locales subbed by platinum

iotas structure is detached contamination energy levels over the valence band, as indicated by the debasement energy level. The UV light energizes electrons in both the VB and pollution energy levels when illuminated, However, apparent light can just energize electrons at the debasement energy level. Oxygen opening reasoned that, oxygen-lacking destinations made at grain limits are fundamental for movement to arise, and platinum-doped oxygen-inadequate locales are significant as a re-oxidation blocker. **Morawski *et al.* (2005)**, **Nolan *et al.* (2008)** and **Bayikadi *et al.* (2020)** obtained the Pt-doped TiO₂ via direct heat treatment of TiO₂.xH₂O at temperatures of 373-1073 K under an ammonia atmosphere. The UV-Vis/DR spectra of Pt-doped TiO₂ catalysts showed an additional absorption edge in the visible region ($\lambda \approx 470$ nm; $E_g \approx 2.64$ eV) at temperature higher than 673 K. Based on XRD investigation, it may be assumed that Pt-doping didn't affect the anatase-to-rutile stage change. The photoactivity of the adjusted impetuses was resolved based on disintegration pace of phenol and azo-stain (Reactive Red 198) when exposed to visible light. The most photoactive catalysts for azo-dye degradation were those calcined at 773 and 873 K (about 40-45 percent), while catalysts calcined at 973 K resulted in phenol decomposition (6.55 percent). Those could be the result of distinct photodegradation mechanisms for the chemicals (**Moza *et al.*, 2005**; **Bayikadi *et al.*, 2020**).

The present study was organized to utilize a portion of the Pt-doped TiO₂ in photocatalytic debasement of phenol. Likewise, the photocatalytic activities and rate constants of every Pt-doped TiO₂ and P25 TiO₂ were considered.

MATERIALS AND METHODS

To produce Pt_{ion}-TiO₂, a sol-gel technique was used. A drop-by expansion of approx. 1.25 mL (0.08 mM for 0.5 iota percent Pt doping), with a pH alteration of 1.5 with nitric corrosive arrangement broke down into 25 mL of suprême ethanol to 250 mL (0.25 iota percent Pt doping). The succeeding colloidal suspension was blended at 50 degrees Celsius before the rotating vapor disappeared. Under warm temperatures (between 373 and 873 K), the powder was calcinated. The powder was formed in the absence of chloroplatinic corrosive, non-opted TiO₂. The powder of calcined TiO₂, containing chlorides and nitrate, was cleaned and dried to wipe away contaminants. Pt₀/TiO₂ was prearranged and compared to Pt_{ion}-TiO₂ (TiO₂ metal-saved Pt). Using a photo affidavit approach, Pt₀/TiO₂ was made: TiO₂ (0,5 g/L in the preceding manner of powder suspension) was unoped by a mercury light of 200-W with 1M methanol (electron donor) and 30 μ M chloroplastic acid for a period of 30 minutes (H₂PtCl₆) Pt-deposited TiO₂ after irradiation, then powder was removed, cleaned and airdried. Pt-chloride-sensitized TiO₂ (PtCl_x/TiO₂) was formed by applying 30 mM H₂PtCl₆ to an undoped TiO₂ suspension (0.5 g/L, as mentioned above), at the water was dissipated and airdried. The anatase network was shared by the Pt_{ion}-TiO₂, Pt₀/TiO₂, and PtCl_x/ TiO₂ in this analysis, synthesized and compared. Degussa P25, a combination of anatase and rutile, as a good starting point (8:2), was also used (**Kim *et al.*, 2005**; **Moza *et al.*, 2005**; **Wdaah Alsalih, 2019**) and displayed as follows:

XRD

Diffractometer with monochromatic, high-intensity Cu K diffractometer ($\mu = 0.154056$ nm), Holland Philips Xpert +2"/min from 10" to 60" (2 vol) (2 (2 θ)).(Wdaah Alsalih, 2019).

AFM

It is a mechanism used to determine or photograph the particles and also to determine the volume of three-dimensional, x, y and z particles. Apprehension suspected A Qualified Inc. in the United States. Sample 3000A model microscope.

ATR-FTIR , UV-Vis

ATR-FTIR Bruker Model Tensor 27, Uv- Visible Spectrophotometer, PG instrument Ltd ,double+90Plus.

RESULTS

Synthesized compounds (Pt- doped TiO_2) were characterized. A Holland Philips Xpert X-ray powder diffraction (XRD) was utilized for the phase identification of crystalline nanoparticles that provide information on unit particles dimensions. A diffractometer was used to characterize the synthesized nano- TiO_2 (anatase) and nano- Pt- doped TiO_2 particles using XRD and AFM, as shown in Figs. (1),(a) and (b). The x-ray diffraction revealed the following as compared to the regular result.

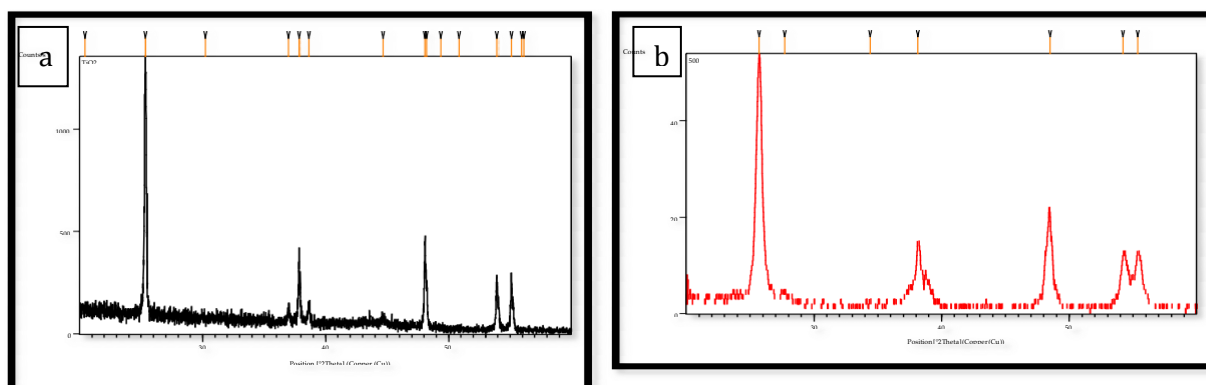


Fig. 1: (a) XRD pattern for TiO_2 (anatase). **Fig. 1: (b)** XRD pattern for Pt- doped TiO_2 .

Fig (1-a) demonstrates X-ray diffraction for TiO_2 (anatase) from this figure the main peak was noticed at $2\theta=25.3455$, the intensity was 100% and peaks were at $2\theta=37.8298, 48.0772, 53.9206, 55.1004$. Fig (1-b) represents a XRD for Pt- doped TiO_2 ,

the main peak was noticed at ($2\theta = 25.7175$) with intensity 100 % and peaks at $2\theta = 38.1511, 48.4860, 54.2079, 55.3687$.

The size distribution of minutes between 60- 135nm for TiO_2 (anatase) and the size distribution of minutes between 50- 150nm for Pt- doped TiO_2 were prepared at 873k and indicated by AFM spectra. The findings showed that, Pt-doped TiO_2 had the largest surface area, followed by TiO_2 (anatase), which had the smallest surface area as particle size decreases. The outcome corresponded with the reviewers who affirmed this claim (**Kim *et al.*, 2005; Bayikadi *et al.*, 2020**) that is illustrated in following Figs.(2) and (3).

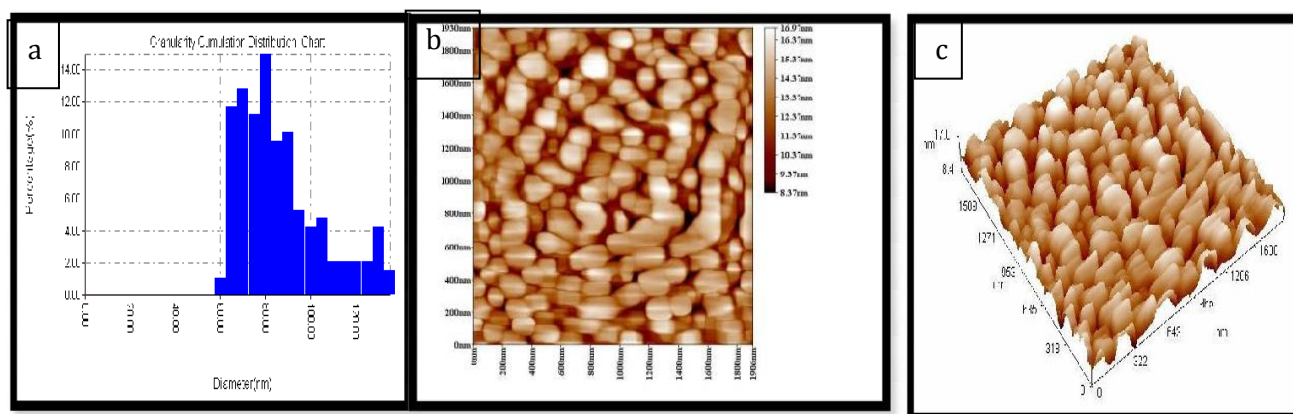


Fig. 2: (a) size distribution for catalyst TiO_2 (anatase) particle by AFM. (b) prepared particles sketched on X-Y axis catalyst TiO_2 (anatase) by AFM. (c) prepared particles sketched on X-Y-Z axis for catalyst TiO_2 (anatase) by AFM.

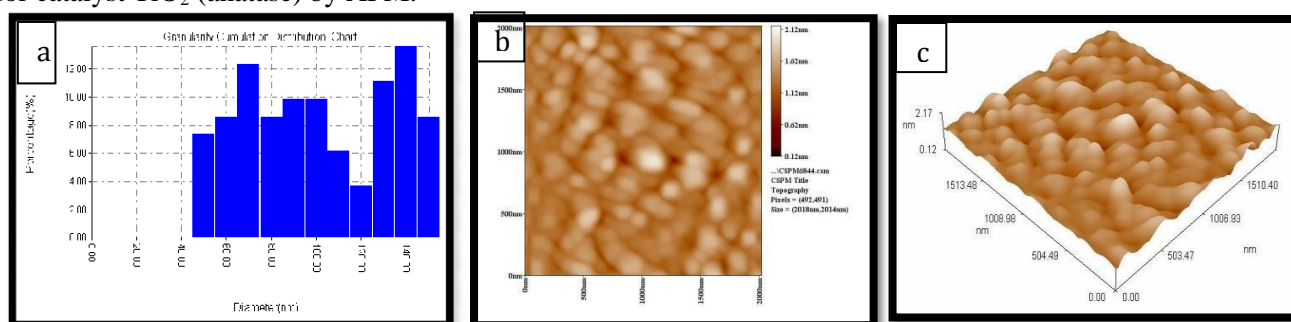


Fig. 3: (a) size distribution for catalyst Pt- doped TiO_2 particle by AFM. (b) prepared particles sketched on X-Y axis for catalyst Pt- doped TiO_2 by AFM. (c) prepared particles sketched on X-Y-Z axis for catalyst Pt- doped TiO_2 by AFM.

ATR-FTIR spectrum

The results showed that low frequency bands were 500cm^{-1} that corresponded to the vibration of Ti-O-Ti bond for catalyst TiO_2 (anatase) as presented in Fig (4).

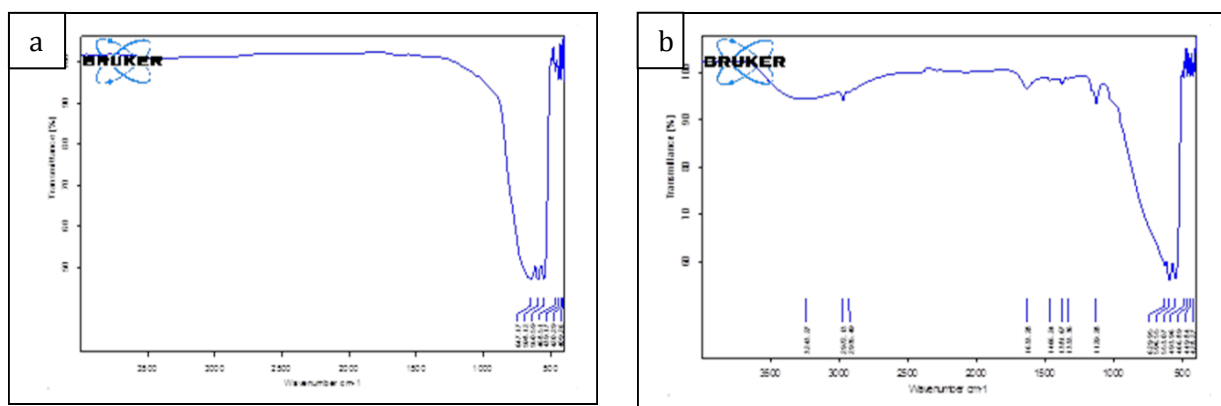


Fig. 4: (a) ATR-FTIR spectrum of catalyst TiO_2 (anatase). (b) ATR-FTIR spectrum of catalyst Pt- doped TiO_2 .

Fig. (4) shows a Pt-doped TiO_2 catalyst with a dried temperature of 120°C . Peaks of water and hydroxylic groups can be attributed to a range of 3243 to 1633 cm^{-1} , whereas platinum atoms replaced with a TiO_2 array may be credited to the peak of 1438 cm^{-1} , which comes from the N-H bending (Hashimoto et al., 2005; Paramasivam et al., 2012).

2.1 UV-Vis absorption spectra

The wavelength in the UV-visible spectra was the uptake of the N-doped- TiO_2 catalyst, which marked the end of the straight line in the spectrum (Rashed and El-Amin, 2007) as shown in Fig. (5) according to the relationship of Planck's law.

Table 2: Energy band gap (E_g).

Type of catalyst	λ (nm)	E_g (Joules) $\times 10^{-19}$	E_g (eV)
TiO_2 (anatase)	384	5.2	3.2
Pt-doped TiO_2	482	4.1	2.5

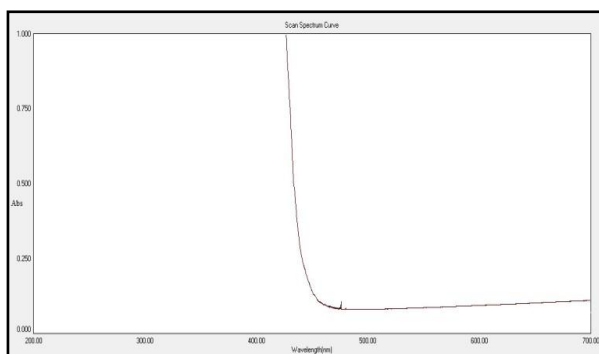
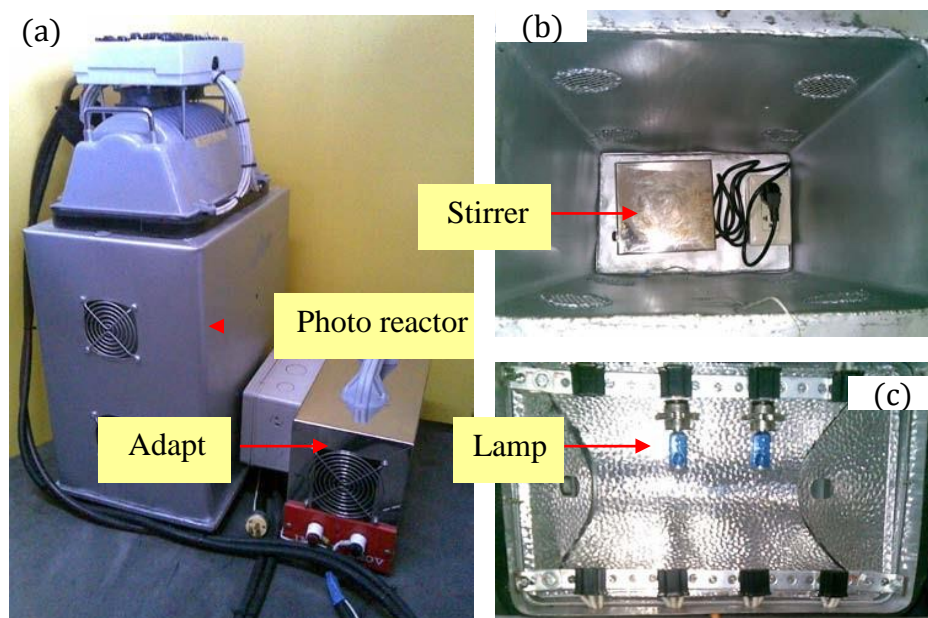


Fig. 5: Uv-visible spectra of catalyst Pt- doped TiO_2 .

Inventive photo reactor

Using an ingenious photo reactor, the photo degradation reaction of phenol was investigated (Fig. 6). A 90/100W Xe lamp was installed as a light source, with the ability to work at 90W, 100W, or 190W per lamp. The conversion of AC 220V to DC 12V required the use of a



current adaptor. There was a collection of magnetic stirrers inside the reactor, as well as a 400 ml foil-covered beaker with a HOYA UV 385 cutoff filter. Furthermore, during the 9-hour reaction, this reactor was assumed to maintain a temperature of 303 K within the reactor.

Fig. 6: The imaginative photo reactor is depicted graphically as follows: (a) the photo reactor set, (b) the stirrer set, and (c) the lamp set. The general method for studying the photocatalytic activity of each photo catalyst is as follows:

DISCUSSION

The following is a general method for determining each photo catalyst's photocatalytic activity:

Immediately, a 400 ml foil-covered beaker with a UV cutoff filter was filled with 125.00 ml of 20 ppm phenol separated from 500 ml of 20 ppm phenol. The photo catalyst was then applied at a concentration of 0.1000 g (0.8000 g/l). The degradation reaction was run in the dark for an hour before being switched to artificial light with a 190 W Xe-lamp. The dark reaction was carried out in order to get the system to equilibrium until it degraded. During the time of degradation, the solution was stirred in the photo reactor at a constant temperature (303 K). the results corispondance with each rearschers (**Rappoport, 2004; Karim and Fakhruddin, 2012; Darabdhara *et al.*, 2016; Dimkpa *et al.*, 2018; Levchuk *et al.*, 2018; Das *et al.*, 2020**).

The sampling of the initial level (before adding a photo catalyst) and the remaining levels of phenol in each length of time was used in the follow-up to the reaction by hypodermal

syringes. The stirrer was turned off for 15 minutes before the samples were collected to prevent the catalyst from being suspended in the solution. All of the collected samples were left in the dark overnight before being centrifuged for around 30 minutes to minimize the fine-powdered catalyst's distribution. The centrifugation was then moved into a vial using a dropper. Finally, all samples were diluted to a specific amount with distilled water, and their concentrations were determined using the required specific methods for photo degradation of phenol. This part also employed Pt-doped TiO_2 which was prepared by titanium(IV) tetraisopropoxide mixed with H_2PtCl_6 and calcined at 673 K as a photocatalyst.

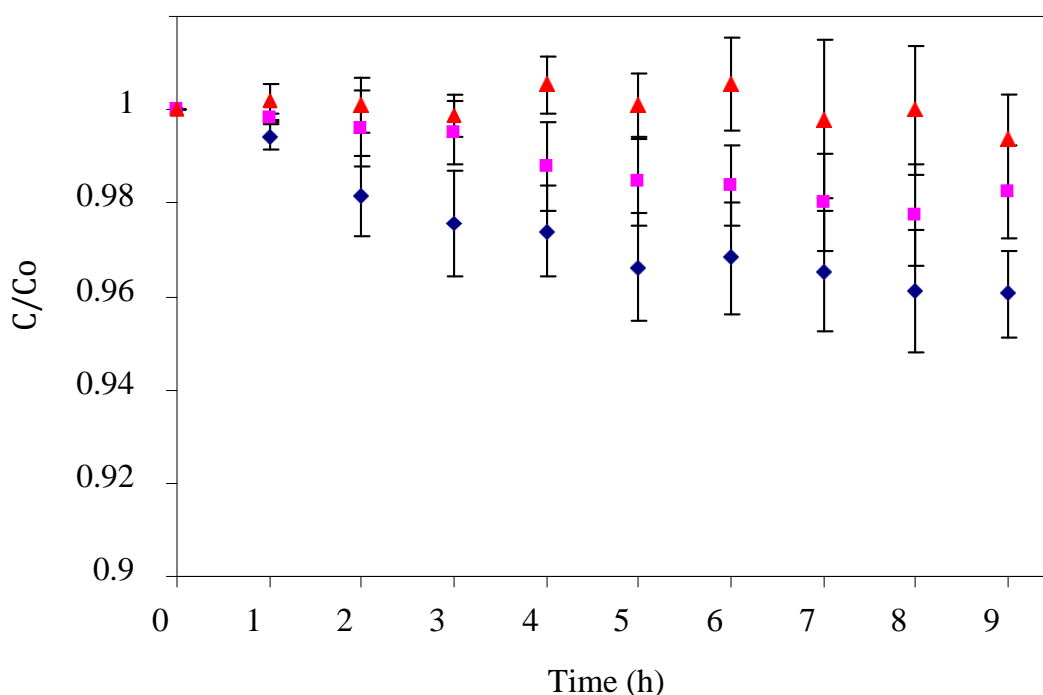


Fig. 7: Photo degradation of phenol by using; (a) Pt-doped TiO_2 calcined at 673 K (◆), (b) P25 TiO_2 (■) and (c) without catalysts (▲).

As shown in Fig. (7), the findings revealed that photographing degradation by Pt-doped TiO_2 could detect only 4 percent of phenol conversion while P25 agrees with that of **Spath and Dayton (2003)**, **Zhang *et al.* (2015)**, **Dimkpa *et al.* (2018)**, and **Vrdhan *et al.* (2019)**.

2 % conversion was provided by TiO_2 . The rate of degrading of both photo catalysts was very slow, as shown in Table (2) due to their rate constants. Those findings show that the mineralization of phenol by that photo catalyst is too difficult. (**Hoffman *et al.*, 1994**; **Hashimoto *et al.*, 2005**; **Bagheri *et al.*, 2014**; **Sun *et al.*, 2020**; **Ijaz and Zafar, 2021**).

In the event of no catalyst, the thermal effect was only 0.6% phenol conversion.

This is why it is possible to ignore the effect of thermal decomposition. In the case of the other substrates, photo degradation rate constants with the whole range of irradiation time could be found: Benz[a]anthracene and 1-5 h, 1-9 h for phenol as illustrated in Figs. (7) and (8).

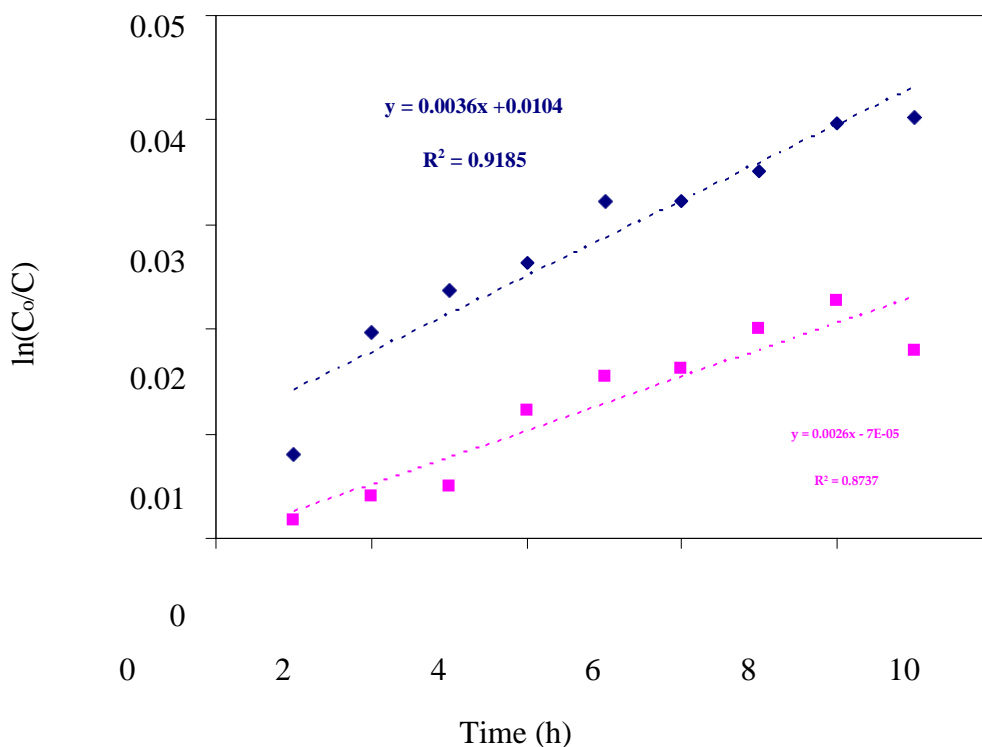


Fig. 8: The relation between $\ln C_0/C$ and time (h) of photodegradation reaction of phenol by (a) Pt-doped TiO_2 using titanium(IV) tetraisopropoxide mixed with H_2PtCl_6 and calcined at 673 K (♦) and (b) P25- TiO_2 (■).

TiO_2 Pt-doped photodegradation successfully applied for phenol removal samples of water at laboratory level, 98.9 percent of phenol was removed after only one passage through the picture with pt-doped TiO_2 in experiments dissolving phenol in bidistilled water.

Exhibition of most of those compounds have been removed under similar experiments with phenol and 2,4-dichlorophenol (99.8 % 98.9 % , respectively). The same phenol dissolved readings were 80.0 and 83.3 percent for two distinct water samples from the Euphrates River. While the initial results for phenol removal from water are promising, additional experiments are required to optimize water treatment conditions in this new model of solid state nanoparticles including photo degradation by Pt-doped TiO_2 generator (exploration period, dissolved photo degradation by Pt-doped TiO_2 , Water flow rate, photo deterioration by one or more water passes, etc.).

CONCLUSION

Photocatalysts are apparent in visible light and are dynamic. The Pt-ion-TiO₂ was used in the current study as another type of apparent light dynamic photocatalyst and demonstrated its apparent mobility in a variety of methods. While Pt-metal-stacked TiO₂ has received a lot of attention as a photocatalyst, Pt-particle doped TiO₂ with apparent light mobility has received less attention. The apparent light ingestion by Pt_{ion}-TiO₂ is credited with the electrical advance between the band edge (CB or VB) and the deformed redox regions of Pt particles subs into the TiO₂ cross-section. The fundamental oxidation provinces of Pt particles in the TiO₂ mass grid were Pt(IV), with some Pt(II) species on a superficial level. Apart from Iraq, Egypt, and South Africa, the number of water quality stations is limited, and pesticides and hazardous metals examinations are rare. Except in Nigeria, Egypt, and Iraq, the effects of industrial development are likely to be limited to the major towns. When polluted places are documented, they indicate contamination levels that match global records, such as for particular metals that get megacities (millions of people) and industrial wastewaters. In response to this demand, new nanocomposite models can be broadly defined as less expensive, simpler to use and environmentally friendly. Overall, as a new visible light active photocatalyst such as nitrogen-doped TiO₂ and carbon-doped TiO₂, Pt_{ion}-TiO₂ was proved to offer great potential.

REFERENCES

- Abbas, A. A. and Hassan, F. M.** (2018). Water quality assessment of Euphrates river in Qadisiyah province (Diwaniyah river), Iraq. *The Iraqi Journal of Agricultural Science*, 49(2):251-261.
- Abdullah, E. J.** (2013). Evaluation of surface water quality indices for heavy metals of Diyala River-Iraq. *Journal of Natural Sciences Research*, 3(8).
- Bagheri, S.; Muhd Julkapli, N. and Bee Abd Hamid, S.** (2014). Titanium dioxide as a catalyst support in heterogeneous catalysis. *The Scientific World Journal*.
- Bayikadi, K. S.; Wu, C. T.; Chen, L.-C.; Chen, K.-H.; Chou, F.-C., and Sankar, R.** (2020). Synergistic optimization of thermoelectric performance of Sb doped GeTe with a strained domain and domain boundaries. *Journal of Materials Chemistry A*, 8(10):5332–5341.
- Black, M.** (2016). *The atlas of water: mapping the World's most critical resource*. Univ of California Press.
- Chenier, P. J.** (2012). *Survey of industrial chemistry*. Springer Science and Business Media.
- Cukrov, N.; Tepic, N.; Omanović, D.; Logen S, Bura-Nakić S, Vojvodic, E., et al** (2012).

Qualitative interpretation of physico-chemical and isotopic parameters in the Krka River (Croatia) assessed by multivariate statistical analysis. *Int J Environ Anal Chem* 92(10):1187–1199

Darabdhara, G.; Boruah, P. K.; Borthakur, P.; Hussain, N.; Das, M. R.; Ahamad, T.; Alshehri, S. M.; Malgras, V.; Wu, K. C.-W. and Yamauchi, Y. (2016). Reduced graphene oxide nanosheets decorated with Au–Pd bimetallic alloy nanoparticles towards efficient photocatalytic degradation of phenolic compounds in water. *Nanoscale*, 8(15): 8276–8287.

Das, T. K.; Sakthivel, T. S.; Jeyaranjan, A.; Seal, S.; and Bezbaruah, A. N. (2020). Ultra-high arsenic adsorption by graphene oxide iron nanohybrid: Removal mechanisms and potential applications. *Chemosphere*, 253: 126702.

Dimkpa, C. O.; Singh, U.; Bindraban, P. S.; Elmer, W. H.; Gardea-Torresdey, J. L. and White, J. C. (2018). Exposure to weathered and fresh nanoparticle and ionic Zn in soil promotes grain yield and modulates nutrient acquisition in wheat (*Triticum aestivum* L.). *Journal of Agricultural and Food Chemistry*, 66(37): 9645–9656.

Ewaid, S. H. and Abed, S. A. (2017). Water quality index for Al-Gharraf river, southern Iraq. *The Egyptian Journal of Aquatic Research*, 43(2): 117-122.

Gönüllü, Y.; Haidry, A. A. and Saruhan, B. (2015). Nanotubular Cr-doped TiO₂ for use as high-temperature NO₂ gas sensor. *Sensors and Actuators B: Chemical*, 217: 78-87.

Hashimoto, K.; Irie, H., and Fujishima, A. (2005). TiO₂ photocatalysis: a historical overview and future prospects. *Japanese Journal of Applied Physics*, 44(12R): 8269.

Hoffman, A. J.; Carraway, E. R. and Hoffmann, M. R. (1994). Photocatalytic production of H₂O₂ and organic peroxides on quantum-sized semiconductor colloids. *Environmental Science and Technology*, 28(5): 776–785.

Hu, J.; Qiao, Y.; Zhou, L. and Li, S. (2011). Spatiotemporal distributions of nutrients in the downstream from Gezhouba Dam in Yangtze River, China. *Environ Sci Pollut Res* 19:2849–285.

Ijaz, M. and Zafar, M. (2021). Titanium dioxide nanostructures as efficient photocatalyst: Progress, challenges and perspective. *International Journal of Energy Research*, 45(3): 3569–3589.

Karim, F. and Fakhruddin, A. N. M. (2012). Recent advances in the development of biosensor for phenol: a review. *Reviews in Environmental Science and Bio/Technology*, 11(3): 261–274.

Kim, S.; Hwang, S.-J. and Choi, W. (2005). Visible light active platinum-ion-doped TiO₂ photocatalyst. *The Journal of Physical Chemistry B*, 109(51): 24260–24267.

Levchuk, I.; Mårquez, J. J. R. and Sillanpää, M. (2018). Removal of natural organic

matter (NOM) from water by ion exchange--a review. *Chemosphere*, 192: 90–104.

Majno, G. (1991). *The healing hand: man and wound in the ancient world*. Harvard University Press.

Mandal, P.; Upadhyay, R. and Hasan, A. (2010). Seasonal and spatial variation of Yamuna River water quality in Delhi, India. *Environ Monit Assess* 170(1):661–670

McGarigal, K.; Cushman, S. A. and Stafford, S. (2013). *Multivariate statistics for wildlife and ecology research*. Springer Science and Business Media.

Moza, S.; Tomaszewska, M. and Morawski, A. W. (2005). Photocatalytic degradation of azo-dye Acid Red 18. *Desalination*, 185(1–3): 449–456.

Mustapha, A. and Nabegu, A.B. (2011) Surface water pollution source identification using principal component analysis and factor analysis in Getsi River, Kano, Nigeria. *Austr J Basic Appl Sci* 5:1507–1512

Nolan, M.; Elliott, S. D.; Mulley, J. S.; Bennett, R. A.; Basham, M. and Mulheran, P. (2008). Electronic structure of point defects in controlled self-doping of the TiO₂ (110) surface: Combined photoemission spectroscopy and density functional theory study. *Physical Review B*, 77(23): 235424.

Pan, C. C. and Wu, J. C. (2006). Visible-light response Cr-doped TiO₂– XNX photocatalysts. *Materials Chemistry and Physics*, 100(1): 102-107.

Pan, Y.; Liu, Y.; Lin, Y. and Liu, C. (2016). Metal doping effect of the M–Co₂P/Nitrogen-Doped carbon nanotubes (M= Fe, Ni, Cu) hydrogen evolution hybrid catalysts. *ACS applied materials and interfaces*, 8(22):13890-13901.

Paramasivam, I.; Jha, H.; Liu, N. and Schmuki, P. (2012). A review of photocatalysis using self-organized TiO₂ nanotubes and other ordered oxide nanostructures. *Small*, 8(20): 3073–3103.

Pradhan, U.K.; Shirodkar, P.V. and Sahu, B.K. (2009). Physico-chemical characteristics of the coastal water off Devi estuary, Orissa and evaluation of its seasonal changes using chemometric techniques. *Curr Sci* 96(9):1203–1209.

Rappoport, Z. (2004). *The chemistry of phenols*. John Wiley and Sons.

Rashed, M. N. and El-Amin, A. A. (2007). Photocatalytic degradation of methyl orange in aqueous TiO₂ under different solar irradiation sources. *International Journal of Physical Sciences*, 2(3): 73–81.

Schulze, T. F. and Schmidt, T. W. (2015). Photochemical upconversion: present status and prospects for its application to solar energy conversion. *Energy and Environmental*

Science, 8(1): 103–125.

- Shrestha, S; Kazama, F. and Nakamura, T.** (2008). Use of principal component analysis, factor analysis and discriminant analysis to evaluate spatial and temporal variations in water quality of the Mekong River. *J Hydroinform* 10(1):43–56
- Singh, K.P.; Malik, A.; Mohan, D.; Sinha, S and Singh, V.K.** (2005). Chemo metric data analysis of pollutants in wastewater: a case study. *Anal Chim Acta* 532(1):15–25
- Spath, P. L. and Dayton, D. C.** (2003). *Preliminary screening--technical and economic assessment of synthesis gas to fuels and chemicals with emphasis on the potential for biomass-derived syngas.*
- Sun, M.; Liu, H.; Sun, Z. and Li, W.** (2020). Donor-acceptor codoping effects on tuned visible light response of TiO₂. *Journal of Environmental Chemical Engineering*, 104168.
- Tobiszewski, M.; Tsakovski, S.;Simeonov, V. and Namieśnik, J.** (2010). Surface water quality assessment by the use of combination of multivariate statistical classification and expert information. *Chemosphere*, 80(7): 740-746.
- Vardhan, K. H.; Kumar, P. S. and Panda, R. C.** (2019). A review on heavy metal pollution, toxicity and remedial measures: Current trends and future perspectives. *Journal of Molecular Liquids*, 290: 111197.
- Vione, D.; Encinas, A.; Fabbri, D. and Calza, P.** (2018). A model assessment of the potential of river water to induce the photochemical attenuation of pharmaceuticals downstream of a wastewater treatment plant (Gadiana River, Badajoz, Spain). *Chemosphere*, 198: 473-481.
- Vittori, A.L.; Trivisano, C.; Gessa, C.; Gherardi, M.; Simoni, A.; Vianello, G., et al.,** (2010) Quality of municipal wastewater compared to surface waters of the river and artificial canal network in different areas of the eastern Po Valley (Italy). *Water Qual Expo Health* 2(1):1–13 .
- wdaah Alsalih, M.** (2019). MODIFICATION OF THE NANO TITANIUM BAND GAP REACTIONS OF SOLID DIOXIDE WITH (ANTIMONY) STIBIUM S AND ITS DETERMINATION PHOTOCATALYTIC ACTIVITY. *Science Proceedings Series*, 1(2): 161–164.
- Wu, Y.; Tao, X.; Qing, Y.; Xu, H.; Yang, F.; Luo, S.; ... and Lu, X.** (2019). Cr- Doped FeNi–P Nanoparticles Encapsulated into N- Doped Carbon Nanotube as a Robust Bifunctional Catalyst for Efficient Overall Water Splitting. *Advanced Materials*, 31(15): 1900178
- Yoon, H. Y.; Lee, J. G.; Esposti, L. D.; Iafisco, M.; Kim, P. J.; Shin, S. G.;Jeon, J.-R. and Adamiano, A.** (2020). Synergistic release of crop nutrients and stimulants from hydroxyapatite nanoparticles functionalized with humic substances: toward a

multifunctional nanofertilizer. *ACS Omega*, 5(12): 6598–6610.

Zhang, Q.; Chere, E. K.; McEnaney, K.; Yao, M.; Cao, F.; Ni, Y.; Chen, S.; Opeil, C.; Chen, G. and Ren, Z. (2015). Enhancement of Thermoelectric Performance of n-Type PbSe by Cr Doping with Optimized Carrier Concentration. *Advanced Energy Materials*, 5(8): 1401977.

Zhu, X.;Zhang, D.; Chen, C. J.; Zhang, Q.; Liu, R. S.; Xia, Z. and Lu, X. (2020). Harnessing the interplay of Fe–Ni atom pairs embedded in nitrogen-doped carbon for bifunctional oxygen electrocatalysis. *Nano Energy*, 71: 104597.

المخلص العربي

ضبط فجوة النطاق لثاني أكسيد التيتانيوم وتطبيقه فائدته في التحلل الضوئي لمياه الصرف الصحي (الفينول)

تم العثور على تركيز عالي من الفينول ومشتقاته في المياه السطحية لنهر الفرات في مدينة الناصرية جنوب العراق والتي تسبب في تلوثه بمياه الصرف المشتقة من مواد كيميائية مختلفة. تتضمن هذه الدراسة تعديل فجوة نطاق ثاني أكسيد التيتانيوم بصورة الانتيز, TiO_2 (anatase) عن طريق التحفيز باستخدام ذرات البلاطين باستخدام طريقة "sol-gel". سيقبل التعديل الفجوة التي تفصل مستويات الطاقة بين نطاق التوصيل CB ونطاق التكافؤ VB ، وبالتالي ، يسهل نقل الإلكترونات المثارة من VB إلى CB. إن امتصاص الطاقة من الفوتونات الساقطة التي لها نفس طاقة فجوة الحزمة أو أكبر منها سيعزز تكوين زوجين (فجوة الإلكترون). سوف يعمل الزوجان الناتجان (e^- / h^+) لإنتاج جذور $(\cdot\text{OH})$ تقوم جذور OH^- باكسدة المواد الملوثة لان لها القدرة الكاملة لتدمير الملوثات العضوية في الماء والتي تمتص على سطح التحفيز الضوئي ,تم التحري عن بنية مساحيق TiO_2 المحضرة باستخدام تقنية XRD ، وتم تمييز حجم الجسيمات وتوزيعها باستخدام الفحص المجهرى للقوة الذرية AFM . تمت متابعة التفاعل التحفيزي باستخدام ATR-FTIR و UV-Vis الطيفي. تمت دراسة تأثير وزن المحفز الضوئي TiO_2 من (0.10 - 0.83 جم. لتر -1) لرصد تأثيره على معدل تحلل الفينول على المحلول المائي المحدد مسبقاً للمركب. وجد أن الوزن الأكثر فاعلية يساوي (0.43 جم. لتر -1). ايضا تمت دراسة أنشطة TiO_2 و TiO_2 المخدر مع البلاطين تحت تأثير مصدر للأشعة فوق البنفسجية وأشعة الشمس المباشرة تحت نفس الظروف. أوضحت النتائج أن التفاعل يخضع للحركية من الدرجة الأولى ذات معدل ثابت قدره 4.69×10^{-6} دقيقة⁻¹ لثاني أكسيد التيتانيوم العادي P25 و 9.44×10^{-6} دقيقة ل TiO_2 المحفز بالبلاطين.